

# Ballistic quantum transport in L-shaped Vertical Halo-Implanted $p^+$ -GaSb/InAs n-TFETs

Bhupesh Bishnoi and Bahniman Ghosh

**Abstract**—In the present work, we have investigated ballistic quantum transport in vertical halo-implanted  $p^+$ -GaSb/InAs n-TFETs. We have investigated the current-voltage characteristics, ON-current, OFF-current leakage, subthreshold swing variation as function of gate length, drain length, gate undercut, equivalent oxide thickness, High-K and drain thickness. The electrostatic control, I-V performances and optimization of device structure are carried out for novel L-shaped nonlinear geometry n-TFETs. In the n-TFETs device  $p^+$ -GaSb/InAs heterostructure gives rise to type-III broken gap band alignment. In this geometry the gate electric field and tunnel junction internal field are oriented in same direction and assist the Band-to-Band tunnelling process. To study the ballistic quantum transport in this L-shaped nonlinear geometry we used 3-D, full-band atomistic  $sp^3d^5s^*$  spin-orbital coupled tight-binding method based quantum mechanical simulator which works on the basis of Non-Equilibrium Green Function formalism to solve coupled Poisson-Schrödinger equation self-consistently for potentials and Local Density of state.

**Index Terms**—Band-to-Band tunnelling (BTBT), broken bandgap (BG), Halo-Implanted  $p^+$ -GaSb/InAs heterojunction, Non-Equilibrium Green Function (NEGF), n-tunnel field-effect transistors (n-TFETs).

## I. INTRODUCTION

Intensive research work is going on in TFETs as power-supply scaling below 0.5 V is possible in these devices and at low voltages TFETs can outperform aggressively scaled MOSFETs. Hence, overall power consumption can be reduced in nanoelectronics integrated circuits by using TFETs. [1] In TFETs charge carriers are injected into the channel by band-to-band tunneling (BTBT) process and hence compared to conventional MOSFETs TFETs can have subthreshold swing lesser than 60 mV/decade. [2] In present scenario Tunnel field-effect transistors (TFETs) are promising candidates due to their steep subthreshold swing(SS), better ON to OFF current ratio and high drive current at low voltages operation. In the ITRS 2012 roadmap TFETs operate on  $V_{DD}$  lesser than 0.5 V,  $I_{ON}$  current of 100 milli-amperes,  $I_{ON}/I_{OFF} > 10^5$  and SS below 60 mV per decade.[2] Recently,

Bhupesh Bishnoi is with the Department of Electrical Engineering, Indian Institute of Technology, Kanpur, 208016, INDIA (e-mail: bbishnoi@iitk.ac.in).

Bahniman Ghosh is with the Department of Electrical Engineering, Indian Institute of Technology, Kanpur, 208016, INDIA and Microelectronics Research Center, 10100, Burnet Road, Bldg. 160, University of Texas at Austin, Austin, TX, 78758, USA (e-mail: bghosh@utexas.edu).

new vertical geometry TFETs has been experimentally demonstrated. In this geometry steep subthreshold swing (SS) can be achieved by in line field orientation of gate field and tunnel junction internal field. [3] GaSb/InAs broken-gap (BG) band aligned materials have zero band overlap and narrow band gap of 0.7266 eV and 0.354 eV and are favorable to build TFETs. The GaSb and InAs junction gives type-III broken bandgap alignment which assists the Band-to-Band tunneling (BTBT) process at the junction. [4] In this article, we demonstrate various electrostatic and geometrical considerations that influence the scaling and design of vertical halo-implanted  $p^+$ -GaSb/InAs n-TFETs of 4 nm thin channel structures with gate lengths of 20 nm.

## II. DEVICE STRUCTURE

The vertical halo-implanted  $p^+$ -GaSb/InAs n-TFETs have n-type InAs channel thickness  $T_{InAs}$  of 4 nm with a doping density of  $5 \times 10^{17} \text{ cm}^{-3}$  and 10 nm p-type GaSb source with doping density of  $4 \times 10^{18} \text{ cm}^{-3}$ . Figure 1 shows the cross section cartoon diagram of simulated vertical halo-implanted  $p^+$ -GaSb/InAs n-TFETs structures.

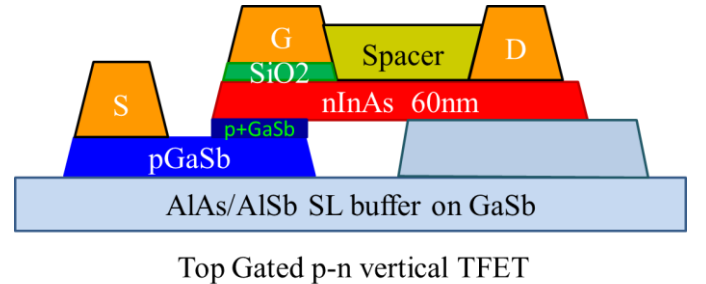


Fig. 1. Cross section cartoon diagram of the simulated vertical halo-implanted  $p^+$ -GaSb/InAs n-TFETs

We have 2 nm halo-implanted  $p^+$ -type GaSb source injector in between source and drain region with doping density of  $4 \times 10^{19} \text{ cm}^{-3}$ . As per ITRS 2012 we performed simulation at 20 nm gate length ( $L_G$ ), 10 nm source length, 60 nm drain length ( $L_D$ ) and 1.9 nm  $\text{SiO}_2$  gate thickness.  $\text{SiO}_2$  spacer of an overlap length ( $L_S$ ) is used to decouple the drain-gate region to reduce ambipolar conduction. Junction length ( $L_J$ ) is length of active tunnelling junction and InAs channel has 10 nm undercut length ( $L_{UC}$ ) which helps to achieve a steep SS. Figure 2 shows the structure of simulated device.



### B. Current-Voltage characteristics

Figure 5 shows the  $I_{DS}$ - $V_{GS}$  transfer characteristics of vertical halo-implanted  $p^+$ -GaSb/InAs n-TFETs at  $V_{DS}$  of 0.3V and 0.03V. In the ON-state condition with  $V_{DS}$  of 0.3 V on applying gate voltage  $V_{GS}$  of 0.6 V, an  $I_{ON}$  current of 100  $\mu A/\mu m$ , an  $I_{ON}/I_{OFF}$  ratio of  $10^{17}$  with subthreshold swing of about 15.34 mV/decade are obtained. In the ON-state for gate voltage  $V_{GS}$  higher than 0.8 V drain current almost saturates and TFET gives high output resistance. In the OFF-state at  $V_{DS}= 0.3$  V, minimum value of drain current is at  $V_{GS}= 0V$ , which indicates that gate has good control in turning off the tunnel junction.

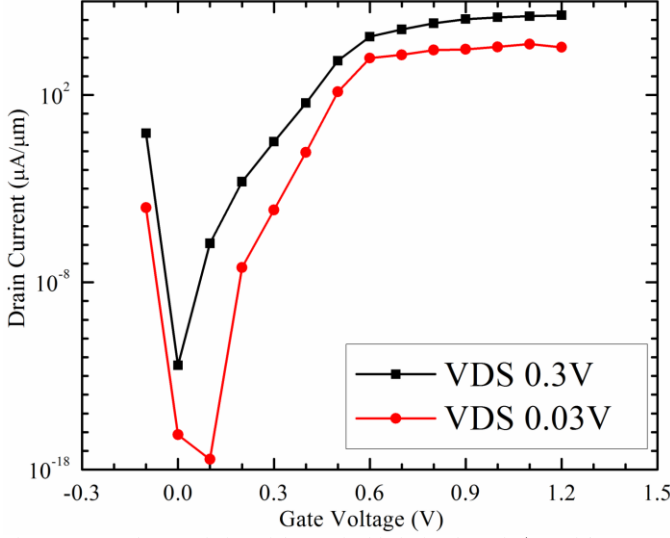


Fig.5  $I_{DS}$ - $V_{GS}$  characteristics of the vertical halo-implanted  $p^+$ -GaSb/InAs n-TFETs at  $V_{DS} = 0.03$  V and  $V_{DS} = 0.3$  V.

Figure 6 shows the  $I_{DS}$ - $V_{DS}$  output characteristics of vertical halo-implanted  $p^+$ -GaSb/InAs n-TFETs at  $V_{GS}$  variation of 0.1 V, 0.2 V, 0.3 V, 0.6 V, 0.9 V and 1.2 V. In the ON state, with drain voltage  $V_{DS}$  of 0.3 V, the entire area of tunnelling junction is turned on and current density is uniform across the junction. For  $V_{GS}$  of 0.1 V the tunnelling current is essentially extinguished and thermionic emission is governed by the leakage current. Figure 7 shows the ON-state  $I_{DS}$ - $V_{GS}$  transfer characteristics with variation of temperature in vertical halo-implanted  $p^+$ -GaSb/InAs n-TFETs. Temperature dependence is found to be considerably weaker in the temperature range of 200K to 300K clearly indicating direct band-to-band tunnelling. For gate voltage of 0.7 V and above, the temperature dependence is extremely minute and current saturates. At 400K we found that the current is an order of magnitude lower than that in the above mentioned temperature range in the gate voltage range of 0.2 V to 0.6 V. For gate voltage larger than 0.7 V current saturates and becomes independent of temperature.

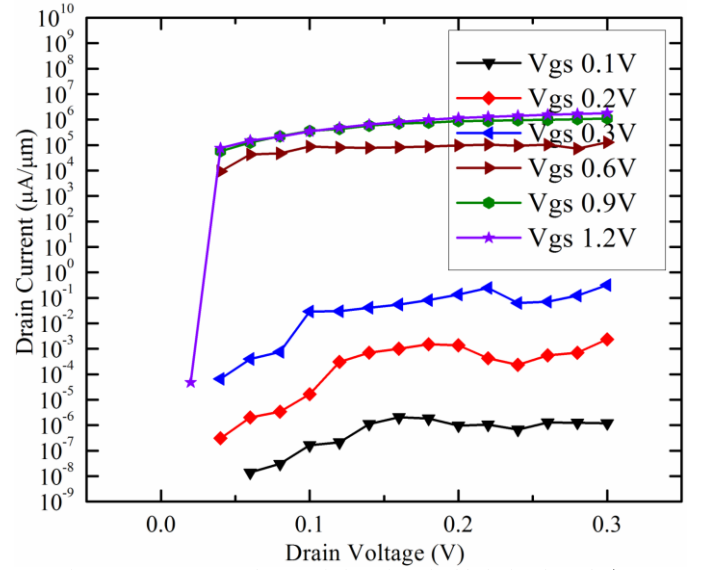


Fig.6  $I_{DS}$ - $V_{DS}$  output characteristics of vertical halo-implanted  $p^+$ -GaSb/InAs n-TFETs with gate voltage variation  $V_{GS}$

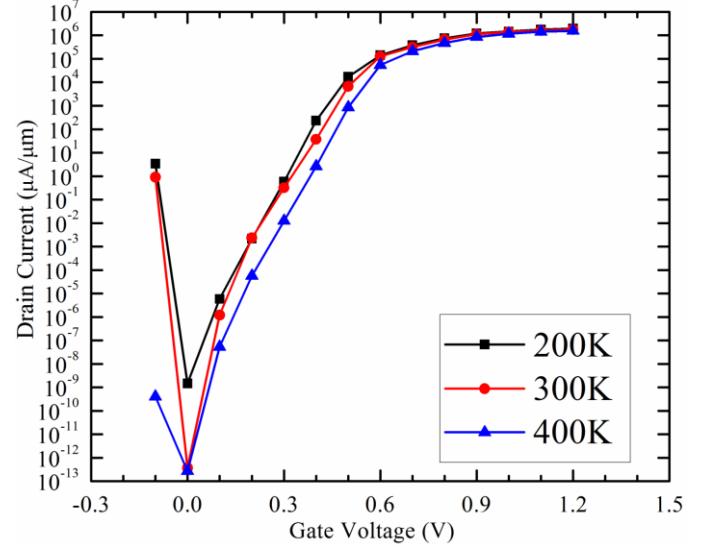


Fig.7.  $I_{DS}$ - $V_{GS}$  characteristics of the vertical halo-implanted  $p^+$ -GaSb/InAs n-TFETs at  $V_{DS} = 0.3$  V with variation in temperature.

### C. Effect of Geometry variation in vertical Halo-Implanted $p^+$ -GaSb/InAs n-TFETs

We investigated five different types of geometric variations and their effect on I-V characteristics of vertical halo-implanted  $p^+$ -GaSb/InAs n-TFETs. Figure 8 shows the ON-state  $I_{DS}$ - $V_{GS}$  transfer characteristics with variation in drain length ( $L_D$ ) in the vertical halo-implanted  $p^+$ -GaSb/InAs n-TFETs. The ambipolar current is estimated in the real devices sense since the simulation includes the quantization effect and effective increase in channel bandgap. Electrostatic effect remains unaffected by the channel quantization and increase in channel bandgap. We observed that increasing the drain length ( $L_D$ ) increases the ambipolar conduction current and hence turn-on characteristics and  $I_{ON}$  current largely increases.

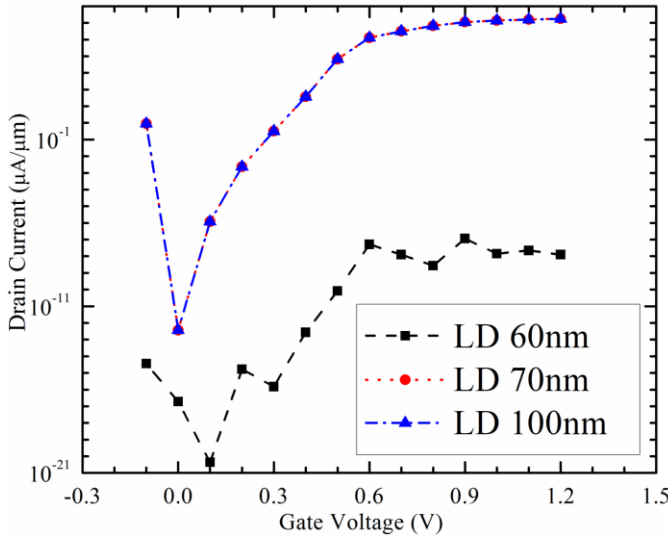


Fig.8.  $I_{DS}$ - $V_{GS}$  characteristics of the vertical halo-implanted  $p^+$ -GaSb/InAs n-TFETs at  $V_{DS}=0.3$  V with variation in drain length ( $L_D$ ).

Figure 9 shows the ON-state  $I_{DS}$ - $V_{GS}$  transfer characteristics with variation in undercut lengths ( $L_{UC}$ ) in the vertical halo-implanted  $p^+$ -GaSb/InAs n-TFETs. For zero undercut length,  $I_{ON}/I_{OFF}$  ratio is reduced by ten orders of magnitude and the subthreshold swing increases to 43.4 mV/decade. Subthreshold swing reduces to 23.7 mV/decade on increasing undercut length to 5 nm and further subthreshold swing reduces to 13.8 mV/decade and  $I_{ON}/I_{OFF}$  ratio increases on increasing the undercut length to 10 nm.  $I_{ON}$  current reduces on further increase in the undercut length as  $I_{ON}$  current is proportional to the tunnel junction area and hence on increasing the undercut length  $L_{UC}$  width-normalized  $I_{ON}$  current density decreases. Here the optimization criterion is overlapping the gate on the tunnelling region. The scalability of vertical halo-implanted  $p^+$ -GaSb/InAs n-TFETs is limited by undercut length  $L_{UC}$  which is necessary to achieve a steep slope.

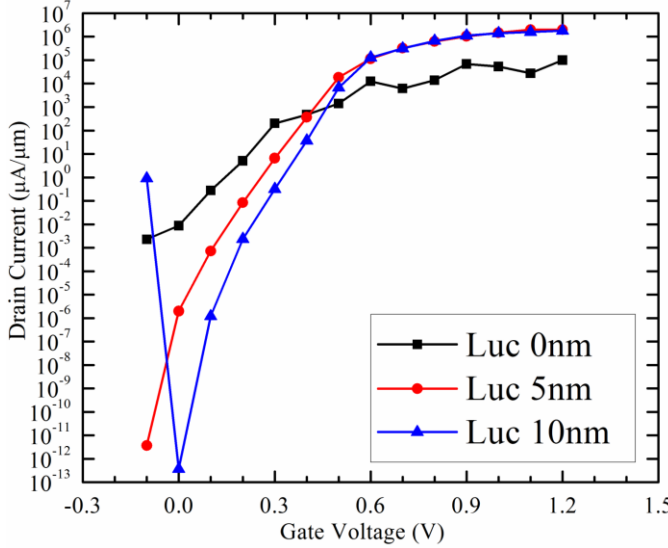


Fig.9.  $I_{DS}$ - $V_{GS}$  characteristics of the vertical halo-implanted  $p^+$ -GaSb/InAs n-TFETs at  $V_{DS}=0.3$  V with variation in undercut length ( $L_{UC}$ )

In the figure 10 we showed the variation of equivalent oxide thickness ( $T_{OX}$ ) on vertical halo-implanted  $p^+$ -GaSb/InAs n-TFETs. A thinner  $T_{OX}$  gives strong coupling between InAs channel and gate field and hence gives rise to steeper

subthreshold swing. With variation in  $T_{OX}$  from 1.2 nm to 4 nm subthreshold swing increases from 13.8 mV/decade to 26 mV/decade. For thinner  $T_{OX}$  due to strong coupling ambipolar current also increases and hence,  $I_{ON}$  current slightly increases. For the vertical halo-implanted  $p^+$ -GaSb/InAs n-TFETs of given undercut lengths ( $L_{UC}$ ) subthreshold slope depends upon the  $T_{OX}$ . In figure 11 we show the variation of different gate oxide material and its impact on the performance of vertical halo-implanted  $p^+$ -GaSb/InAs n-TFETs. For  $Al_2O_3$  High-K gate material subthreshold swing reduces to 12 mV/decade and for  $HfO_2$  High-K gate material subthreshold swing is 13 mV/decade.

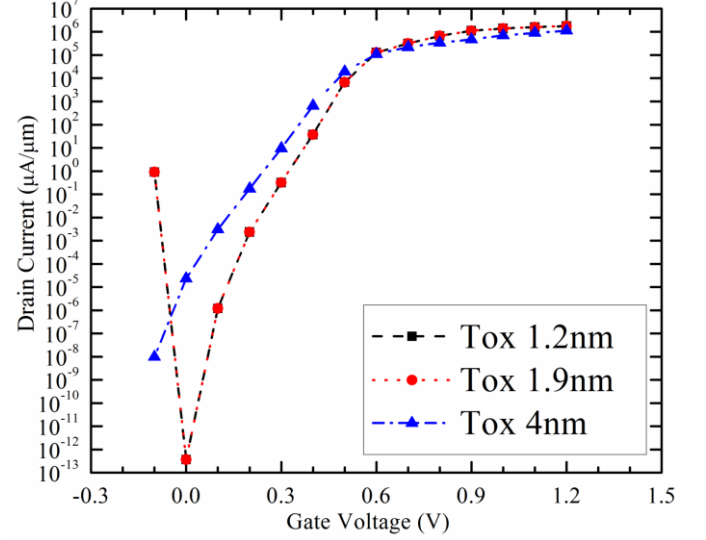


Fig.10.  $I_{DS}$ - $V_{GS}$  characteristics of the vertical halo-implanted  $p^+$ -GaSb/InAs n-TFETs at  $V_{DS}=0.3$  V with variation in  $T_{ox}$ .

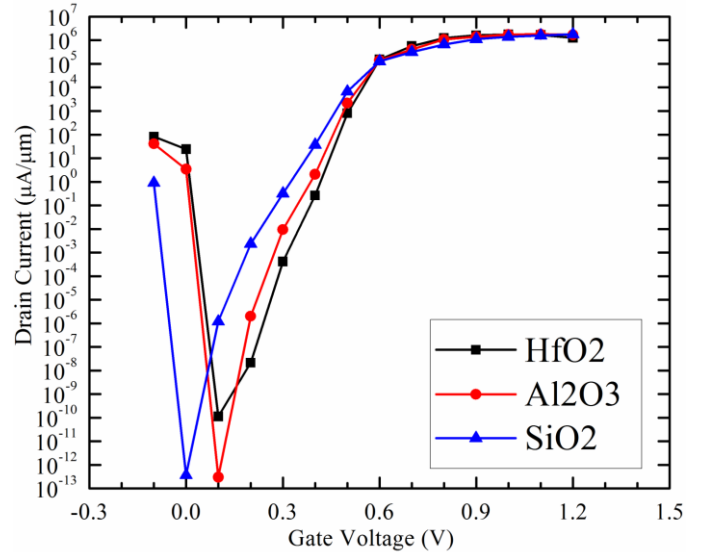


Fig.11.  $I_{DS}$ - $V_{GS}$  characteristics of the vertical halo-implanted  $p^+$ -GaSb/InAs n-TFETs at  $V_{DS}=0.3$  V with variation in gate oxide material.

In figure 12, we show the effect of gate-length ( $L_G$ ) variation on vertical halo-implanted  $p^+$ -GaSb/InAs n-TFETs. We vary the gate lengths ( $L_G$ ) from 10 nm to 30 nm while holding all other geometric parameters constant. Gate length ( $L_G$ ) had a weaker influence on  $I_{OFF}$  current. But, as gate length ( $L_G$ ) increases, overlap over tunnelling junction area also increases and hence  $I_{ON}$  current increases.  $I_{ON}$  current increases with the gate length ( $L_G$ ) from 10 nm to 30 nm. However, gate length

strongly influences subthreshold swing and as gate length decreases subthreshold swing becomes steeper. Simulation results suggest that performance of vertical halo-implanted  $p^+$ -GaSb/InAs n-TFETs is determined by drain-gate periphery and gate has good control at the center of the tunnel junction to turn off the device effectively.

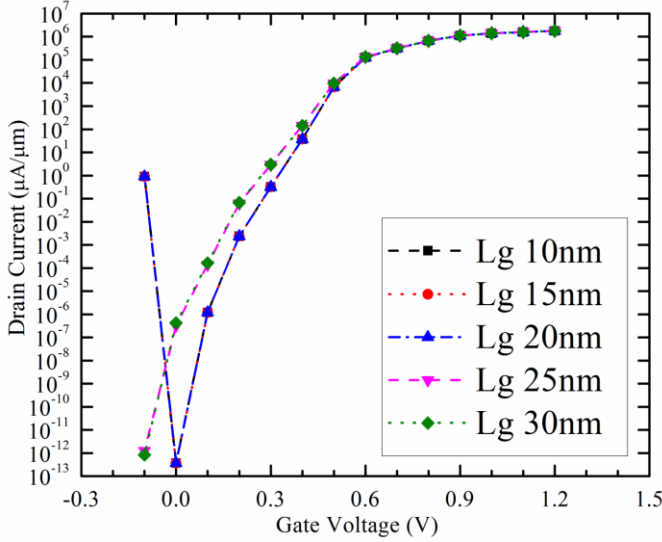


Fig. 12.  $I_{DS}-V_{GS}$  characteristics of the vertical halo-implanted  $p^+$ -GaSb/InAs n-TFETs at  $V_{DS}=0.3$  V with variation in gate length ( $L_G$ )

Figure 13 shows the effect of variation of drain thickness ( $T_{InAs}$ ) in vertical halo-implanted  $p^+$ -GaSb/InAs n-TFETs.  $I_{OFF}$  current and subthreshold slope depend upon the InAs channel thickness ( $T_{InAs}$ ). In the thicker InAs channel TFETs gate lose control on tunnel junction to shut off  $I_{OFF}$  current effectively. We observe that at gate voltage of 0.6 V  $I_{ON}$  current increases by more than two orders of magnitude when drain thickness ( $T_{InAs}$ ) increases from 3 nm to 4 nm but with the overhead of higher value of subthreshold slope. For drain thickness ( $T_{InAs}$ ) of 7 nm, we observe that, at gate voltage of 0.5 V,  $I_{ON}$  current of as high as 1 A/ $\mu$ m is achieved with  $I_{OFF}$  of 0.1  $\mu$ A/ $\mu$ m and subthreshold slope of 31 mV/decade. We also observe that high  $I_{ON}$  current can be achieved by higher InAs concentration but at the cost of higher value of subthreshold slope.

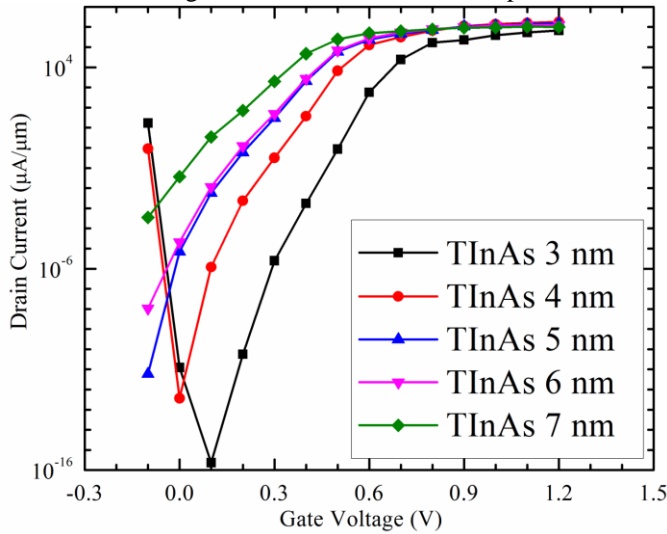


Fig. 13.  $I_{DS}-V_{GS}$  characteristics of the vertical halo-implanted  $p^+$ -GaSb/InAs n-TFETs at  $V_{DS}=0.3$  V with variation in drain thickness ( $T_{InAs}$ ).

Figure 14 shows ON-state  $I_{DS}-V_{GS}$  characteristics of the vertical halo-implanted  $p^+$ -GaSb/InAs n-TFETs with and without  $p^+$ -GaSb halo implant. The effect of  $p^+$ -GaSb halo-implant is clearly visible with increase in  $I_{ON}$  current by 2 orders of magnitude at gate voltage of 0.6V. But, the SS slope increases from 11.85 mV/decade to 15.34 mV/decade.

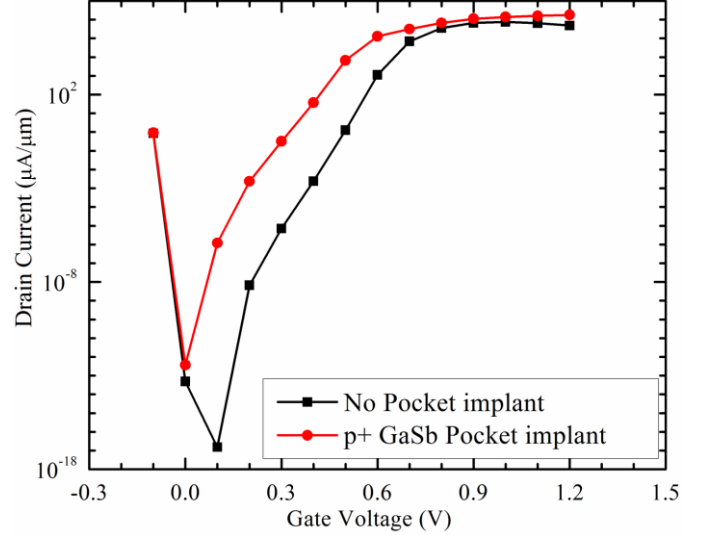


Fig. 14.  $I_{DS}-V_{GS}$  characteristics of the vertical halo-implanted  $p^+$ -GaSb/InAs n-TFETs at  $V_{DS}=0.3$  V with and without  $p^+$ -GaSb halo-implant.

## V. CONCLUSION

Vertical halo-implanted  $p^+$ -GaSb/InAs n-TFETs of 4 nm thin channel structures with the gate lengths of 20 nm have been simulated using a 3-D, full-band, quantum mechanical simulator based on atomistic  $sp^3d^5s^*$  spin-orbital coupled tight-binding method. In the ON-state condition of  $V_{DS}$  0.3 V on applying gate voltage  $V_{GS}$  of 0.6 V, an  $I_{ON}$  current of 100 mA/ $\mu$ m, an  $I_{ON}/I_{OFF}$  ratio of  $10^{17}$  with subthreshold swing of about 15.34 mV/decade are obtained. We investigated five different types of geometric variations and their effects on I-V characteristics of vertical halo-implanted  $p^+$ -GaSb/InAs n-TFETs. These simulation results suggest that the device performance of vertical halo-implanted  $p^+$ -GaSb/InAs n-TFETs is determined by drain-gate periphery and gate length scaling rules do not work for TFETs. Instead other parameters such as channel thickness ( $T_{InAs}$ ), undercut length ( $L_{UC}$ ) and drain length ( $L_D$ ) are critical design parameters for optimization of n-TFETs performance. Simulation results suggest that it is worthwhile to experimentally demonstrate and investigate vertical halo-implanted  $p^+$ -GaSb/InAs n-TFETs in more detail as building block for future low power nano-electronics circuits.

## ACKNOWLEDGEMENT

The authors thank the Department of Science and Technology of the Government of India for partially funding this work.

## REFERENCES

- [1] Sakurai, T., "Perspectives of low power VLSI's." IEICE Trans. Electron, vol. E87-C, no.4, pp. 429-436, 2004.
- [2] Ionescu, Adrian M., and Riel, Heike, "Tunnel field-effect transistors as energy-efficient electronic switches," Nature, vol. 479, no. 7373, pp. 329-337, 2011.

- [3] R. Li, Y. Lu, S. D. Chae, G. Zhou, Q. Liu, C. Chen, M. S. Rahman, T. Vasen, Q. Zhang, P. Fay, T. Kosel, M. Wistey, H. Xing, S. Koswatta, and A. Seabaugh, "InAs/AlGaSb heterojunction tunnel field-effect transistor with tunnelling in-line with the gate field," *Phys. Stat. Solidi (c)*, vol. 9, no. 2, pp. 389-392, 2012.
- [4] Kristijonas Vizbaras, Marcel Törpe, Shamsul Arafin and Markus-Christian Amann, "Ultra-low resistive GaSb/InAs tunnel junctions," *Semiconductor Science and Technology*, vol. 26, no. 7, pp. 075021, 2011.
- [5] Luisier, Mathieu and Klimeck, Gerhard, "Simulation of nanowire tunneling transistors: From the Wentzel-Kramers-Brillouin approximation to full-band phonon-assisted tunneling," *Journal of Applied Physics*, vol. 107, no. 8, pp. 084507, 2010.
- [6] Jancu, Jean-Marc, Scholz, Reinhard, Beltram, Fabio and Bassani, Franco, "Empirical  $sp^3d^5s^*$  tight-binding calculation for cubic semiconductors: General method and material parameters," *Phys. Rev. B*, vol. 57, 11, pp. 6493-6507, 1998.
- [7] Boykin, Timothy B., Klimeck, Gerhard and Oyafuso, Fabiano, "Valence band effective-mass expressions in the  $sp^3d^5s^*$  empirical tight-binding model applied to a Si and Ge parametrization," *Phys. Rev. B*, vol. 69, 11, pp. 115201, 2004.
- [8] Luisier, Mathieu, Schenk, Andreas, Fichtner, Wolfgang and Klimeck, Gerhard, "Atomistic simulation of nanowires in the  $sp^3d^5s^*$  tight-binding formalism: From boundary conditions to strain calculations," *Phys. Rev. B*, vol. 74, 20, pp. 205323, 2006.
- [9] Luisier, Mathieu and Klimeck, Gerhard, "Atomistic full-band simulations of silicon nanowire transistors: Effects of electron-phonon scattering," *Phys. Rev. B*, vol. 80, 15, pp. 155430, 2009.
- [10] Supriyo Datta, "Electronic transport in mesoscopic systems," Cambridge university press, ISBN 0521599431, pp. 393, Cambridge, UK, May 1997.
- [11] Supriyo Datta, "Nanoscale device modeling: the Green's function method," *Superlattices and Microstructures*, vol. 28, no. 4, pp. 253-278, 2000.
- [12] Supriyo Datta, "Quantum transport: atom to transistor," Cambridge university press, ISBN 0521631459, pp. 418, Cambridge, UK, July 2005.
- [13] M. S. Lundstrom, "Fundamentals of Carrier Transport," 2nd ed., Cambridge Univ. Press, ISBN 9780521637244, pp. 440, Cambridge, U.K., July 2009.
- [14] Luisier, M., "A Parallel Implementation of Electron-Phonon Scattering in Nanoelectronic Devices up to 95k Cores," *High Performance Computing, Networking, Storage and Analysis (SC)*, 2010 International Conference for, DOI:10.1109/SC.2010.6, pp. 1-11, 2010
- [15] Zhengping Jiang, Y. He, Yaohua Tan, Michael Povolotsky, Tillmann Kubis, and G Klimeck, "Quantum Transport In GaSb/InAs Nanowire TFET With Semiclassical Charge Density," *International Workshop on Computational Electronics (IWCE)*, May 2012, Madison, WI, 2012.
- [16] Anantram, M. P., Lundstrom, M.S. and Nikonov, D.E., "Modeling of Nanoscale Devices," *Proceedings of the IEEE*, vol. 96, no. 9, pp. 1511-1550, 2008.
- [17] Rahman, Anisur, Guo, Jing, Datta, Supriyo and Lundstrom, M.S., "Theory of ballistic nanotransistors," *Electron Devices, IEEE Transactions on*, vol. 50, no. 9, pp. 1853-1864, 2003.
- [18] Cauley, Stephen, Luisier, Mathieu, Balakrishnan, Venkataramanan, Klimeck, Gerhard and Koh, Cheng-Kok, "Distributed non-equilibrium Green's function algorithms for the simulation of nanoelectronic devices with scattering," *Journal of Applied Physics*, vol. 110, no. 4, pp. 043713, 2011.
- [19] Lake, Roger, Klimeck, Gerhard, Bowen, R. Chris and Jovanovic, Dejan, "Single and multiband modeling of quantum electron transport through layered semiconductor devices," *Journal of Applied Physics*, vol. 81, 12, pp. 7845-7869, 1997.
- [20] Steiger, S., Povolotskyi, Michael, Hong-Hyun Park, Kubis, T. and Klimeck, G., "NEMO5: A Parallel Multiscale Nanoelectronics Modeling Tool," *Nanotechnology, IEEE Transactions on*, vol. 10, no. 6, pp. 1464-1474, 2011.
- [21] AtomistixToolKit version XX.X, QuantumWise A/S.